



A review of articular cartilage and osteoarthritis studies by Fourier transform infrared spectroscopic imaging

Xiao Wang, Mingyang Zhai, Yuan Zhao, Jianhua Yin

Department of Biomedical Engineering, Nanjing University of Aeronautics and Astronautics, Nanjing 210016, China

Contributions: (I) Conception and design: J Yin; (II) Administrative support: None; (III) Provision of study materials or patients: None; (IV) Collection and assembly of data: All authors; (V) Data analysis and interpretation: all authors; (VI) Manuscript writing: All authors; (VII) Final approval of manuscript: All authors.

Correspondence to: Jianhua Yin. Department of Biomedical Engineering, Nanjing University of Aeronautics and Astronautics, Nanjing 210016, China. Email: yin@nuaa.edu.cn.

Abstract: Fourier transform infrared spectroscopic imaging (FTIRI), as a novel and powerful technique, can quantitatively assess and quantitatively predict the spatial structure and chemical composition distribution of complex biological tissues. Furthermore, it can monitor uniquely and quantitatively how diseases correlate with the biochemical composition, distribution and alignment. This work will review the applications and developments of FTIRI in the articular cartilage (AC) and osteoarthritis (OA), which include the structural (anisotropy) detection and content distributions of principal components, the cartilage degeneration and the consequent changes in the structure and the component distribution, evaluation and identification of the healthy and osteoarthritic cartilages at different degeneration stages. It will be helpful for improving our understanding of the complex processes in the variations of molecular composition, distribution and structure even morphology in AC at different degeneration stages, accelerating the early finding, early prevention and effective therapy of cartilage diseases.

Keywords: Fourier transform infrared spectroscopic imaging (FTIRI); osteoarthritis (OA); articular cartilage (AC); collagen; proteoglycan (PG); degeneration

Received: 24 November 2017; Accepted: 09 January 2018; Published: 02 February 2018.

doi: 10.21037/aoj.2018.01.04

View this article at: <http://dx.doi.org/10.21037/aoj.2018.01.04>

Introduction

Articular cartilage (AC) covers the distal aspect of bone in joints to reduce friction and distribute pressure. Two principal macromolecular components in dry AC are type II collagen and proteoglycan (PG), which is saturated with water and mobile ions to constitute of fresh AC (1-3). The collagen fibrils can enmesh PG molecules in its network to maintain the structural integrity of AC by constructing a 3-dimensional fibril network of cartilage. The enmeshed PG with high negative charge density provides the resiliency and compressive strength for AC (4). Histologically, the uncalcified cartilage is conceptually fractionized into three zones including superficial zone (SZ), transitional zone (TZ), and radial zone (RZ) from the surface to tidemark

(1-3,5). The zonal structure is different from the more homogenous nasal cartilage, which is distinguished by the arrangement and shape of chondrocytes, and the fibril orientation (2) that associates with the functional properties of depth-dependent resiliency and tensile strength (6). A few of characteristic changes including the alteration in the collagen fibril structure, PG loss, the size and shape of chondrocytes, and degradation of macromolecules usually forebode the beginning of cartilage degeneration (7), which will eventually lead to cartilage degeneration and osteoarthritis (OA) or other types of arthritis (1).

To effectively determine the structure and concentration distribution of collagen and PG in the tissue from surface to tidemark, therefore, will be helpful for monitoring cartilage degeneration and therapeutic progress. Usually, several

approaches frequently-used to study the structure and principal component content of AC include biochemical analysis (8-10), biomechanical measurement (6,11), micro-magnetic resonance imaging (MRI) (9,10), and some microscopy techniques (11-15). The biochemical and biomechanical methods can't be used to determine the contents of principal components at microscopic level. The μ MRI can't obtain the collagen concentration and distribution in AC yet with an effective MRI protocol. It's very hard for most microscopy techniques (for example, optical microscopy and electron microscopies, etc.) to determine molecular concentrations.

Fourier transform infrared spectroscopic imaging (FTIRI) technique has been a novel and powerful analytical tool with a fine imaging capability. Therefore it has been applied to study the composition variations by combining chemometrics (16) and the structures of biological tissues by integrating with polarization (13) with high spectral resolution and fine spatial resolution that was usually represented with a pixel size on sample image, achieving 3 levels at $50 \mu\text{m} \times 50 \mu\text{m}$, $25 \mu\text{m} \times 25 \mu\text{m}$ and $6.25 \mu\text{m} \times 6.25 \mu\text{m}$, respectively. Additionally, FTIRI combining with chemometrics has shown new applications in biomedical evaluation and identification.

Hence, this review would demonstrate systematically that powerful application of FTIRI in quantitatively assessing pathology-related changes in the composition, distribution and alignment structure of macromolecular principal components, evaluation and identification of healthy and OA cartilages at different degeneration stages. Of course, besides the quantitative analysis, we have to realize that FTIRI (FTIR spectroscopy) has a more special function when it's applied to complex biological systems. That is, it has the possibility to obtain fingerprints of the main biomolecules in sample with single measurement and in a label-free and rapid way, which is impossible achievement for other approaches.

Experimental

Cartilage sample

The cartilage samples and intact knees were usually harvested from special hospitals, animal centers even Slaughterhouse with approval of the institutional review committees. OA samples were usually obtained from osteoarthritic patients or artificial culture with animals. However, the sample preparation in FTIRI is relatively complicated. AC attached on subchondral bones was cut into small blocks (13,16). The blocks were embedded in

water (or paraffin) after washed in saline, then quickly frozen for cutting into thin sections by using cryostat. The sections were rapidly picked up by IR-transmitted crystal plate (BaF₂, ZnSe, ZnS, etc.) or MirrIR slides and (followed washing if embedded by paraffin) dried in air before the FTIRI experiments were performed.

FTIRI and spectroscopy

FTIR imaging system was applied for FTIRI experiments. It included an infrared microscope, an FTIR spectrometer, and a liquid N₂ cooled mercuric cadmium telluride (MCT) array detector. The specimen was mounted on a motor-controlling movable stage in imaging mode, which was located on the focal plane. The AC sections were imaged by the MCT detector at different pixel resolution, for example, 6.25, 25 and 50 μm . The spectral resolution ($1\text{--}32 \text{ cm}^{-1}$) was depended on the experimental requirement over a range of $4,000\text{--}720 \text{ cm}^{-1}$. IR spectra could be extracted from random target pixel or the interested rectangular region, used for spectral analysis. An internal LED illumination was used to get visible images and to rapidly locate region-of-interest (ROI) for IR imaging.

For FTIRI, there were three imaging modes available, including reflection mode, transmission mode and attenuated total reflection (ATR) mode. The corresponding principle diagrams of them were shown in *Figure 1*. Under transmission mode (*Figure 1A*), both of the illumination light and IR beam would enter into the bottom of the IR microscope and pass through the sample. Finally the transmission signals were collected by CCD camera (for visible image) and MCT detector (for FTIR image), respectively. The IR spectra obtained by this mode had the high signal-noise ratio and good spectral quality, while the spectral intensity was easily affected by the thickness and absorbance of sample. Under reflection mode (*Figure 1B*), besides a bottom illumination, a top illumination light and IR beam entered into the IR microscope from its top. The IR signal reflected on sample was collected by MCT detector, as well as visible image recorded by CCD camera. The transmission mode was usually applied in the measurement of transparent sample for IR beam; however, the reflection mode was more commonly used for transparent or not samples, due to the accessibility for the reflection mode. Therefore, it was adopted usually in the IR imaging on AC or OA sections.

A crystal with high reflection index was usually adopted in ATR mode to get higher spatial resolution and richer

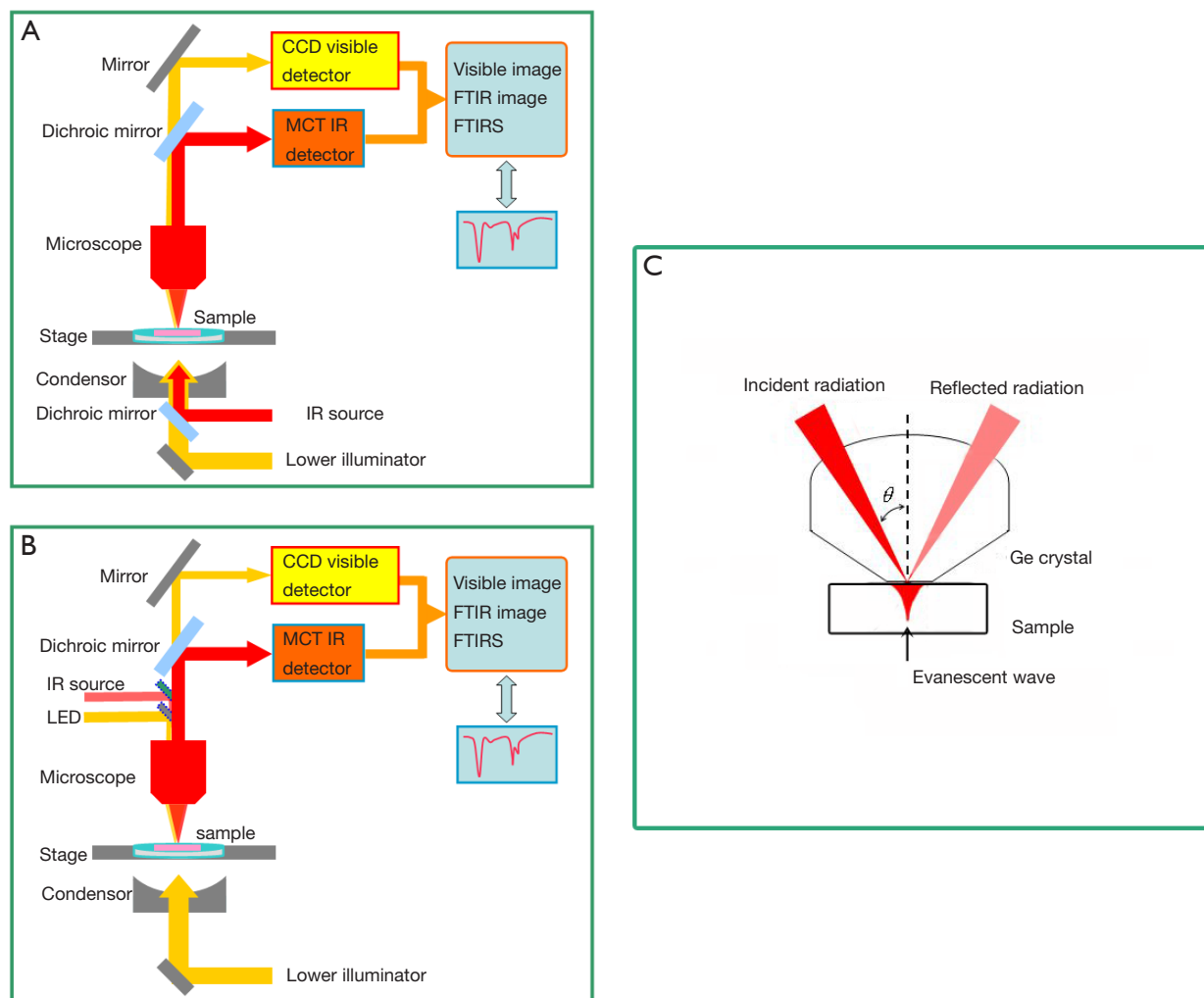


Figure 1 Schematic diagram of 3 imaging modes in FTIRI, including (A) transmission mode, (B) reflection mode, and (C) attenuated total reflection mode. FTIRI, Fourier transform infrared spectroscopic imaging.

structural and morphologic information compared to the other modes. It would be coupled with FTIR microscope, which was followed by the ATR crystal tightly contacting with sample according to ATR principle. ATR mode actually belonged to the reflection category (*Figure 1C*).

Polarized FTIRI have been performed by inserting an infrared wire grid polarizer in incident side or detection side. The FTIR images were recorded at different polarization angles, while the ROI and measurement parameters were not changed. The absorbances of characteristic bands extracted from corresponding chemimaps at different polarization angles were drawn into the angle dependences of characteristic absorbances to express the structural change (13), as well as depth-dependent profiles of the

absorbances at 0° and 90° polarization.

Program of FTIRI research on AC and OC

FTIRI system has been used for cartilage research since 2001 (17). *Figure 2* showed a group of FTIR images with visible image of a health AC section. The research on cartilage imaging can be summarized into three aspects, including structure and content of principal component, and identification/diagnosis of articular disease.

FTIRI for structural change of cartilage (collagen)

FTIRI was used for the preliminary structural analysis on

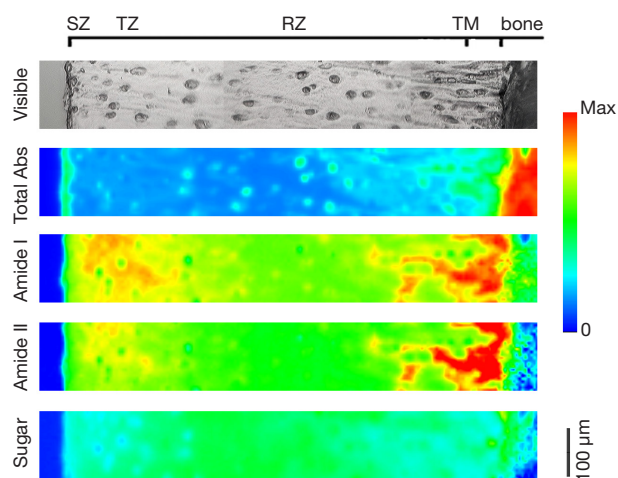


Figure 2 A set of images of a healthy cartilage section including, in turn, visible image, total IR absorption image, amides I and II images, and $1,072\text{ cm}^{-1}$ sugar image, respectively. The color scale with the max absorptions for the FTIR images from the top to the bottom was 1.45, 0.5, 0.35, and 0.30, respectively. The black bar presents 100 microns. SZ, superficial zone; TZ, transitional zone; RZ, radial zone; TM, tidemark; FTIRI, Fourier transform infrared spectroscopic imaging.

the cartilage since 2001 when the FTIRI instrument was just commercialized (17). On the one hand, IR spectra acquired from different locations (zones) of bovine AC reflected the differences in quantity of the principal components (collagen and PG). Besides quantitative analysis of the components in cartilage, the structural analysis was also performed by polarization experiments to determine the spatial orientation of collagen in different zones of AC. It was revealed that the collagen fibril orientation was parallel to the AC surface in SZ, and gradually perpendicular to the AC surface in RZ. This suggested that FTIRI could be used to evaluate the complicated lesion in the tissues with anisotropy.

The orientation of collagen molecules primarily determined the functionality of connective tissues. Therefore, FTIRI integrated polarized technique was established to study the alignment of collagen molecules in AC section, which became popular in the structural research on collagen fiber in histological sections.

FTIRI was utilized to investigate the orientation of collagen molecules in equine AC, in equine repair AC after microfracture treatment, and in human OA cartilage (18). Compared to the polarized light microscopy images of

human OA cartilage, polarized FTIRI showed more obvious zonal identification and orientation, although both of imaging methods revealed similar zonal changes in collagen orientation. The results suggested that the FTIRI method determining molecular orientation changes was prior to their manifestation at the microscopic level (18).

Detailed alignment determinations of collagen fibrils and zonal variations were achieved by Xia's group using polarized FTIRI with dichroism method (19-21). The collagen components of cartilage exhibited anisotropies and alignment changes with the cartilage depth. The absorption profile of amide I was opposite to those of amide II and III, however, both of amide I and II (III) showed the opposite anisotropy in RZ and SZ (13). It was further confirmed that the orientation of collagen in SZ parallel to the cartilage surface became gradually perpendicular to the cartilage surface in RZ. The followed work (22) disclosed that an 'anisotropic flipping' region of collagen orientation located in the TZ for amide I, II and III components.

When the AC was sectioned, parallel to its surface, amide I and II in SZ had the expected infrared anisotropy that was in agreement with that of regular AC sections. For the parallel sections in RZ, however, amide II component showed almost isotropy; in contrast, amide I component showed a distinct anisotropy (23). Anisotropies of amide components enhanced in the perpendicular sections and reduced in the parallel sections when AC depth increased (24).

The further study in Xia's group revealed that, under the external compression, amide II in SZ and amide I in RZ (their bond direction perpendicular to compression direction) retained anisotropy. In contrast, the anisotropy changed significantly for amide I in SZ and amide II in RZ (their bond direction parallel to the compression direction). The depth dependence of the anisotropy under static loading suggested the adaptations of cartilage's morphological structure and chemical distribution (20).

In the perpendicular section, PG component (sugar band) showed a detectable anisotropic flipping at the deep part in the RZ, just above the tidemark, suggesting the orientation of the collagen-attaching PG changed from perpendicular to fibril axis to parallel to fibril axis when the collagen fibrils entered the calcified zone (25).

Rieppo *et al.* (26) investigated the changes in collagen network architecture and collagen content in cartilage during growth and maturation of pigs by the FTIRI. It was revealed that the collagen alignment gradually

Table 1 The characteristic IR bands in cartilage and corresponding assignments (16,17,37)

Centre frequency (cm ⁻¹)	Assignments/Mode
3,330	Amide A: ν_{N-H}
1,660	Amide I: $\nu_{C=O}$
1,560	Amide II: ν_{C-N} , N-H bending
1,338	Proline side chains: CH ₂ wagging vibration
1,240	Amide III: N-H and C-C vibrations
1,072	Glycosylation (sugar) band: C-O-C, C-OH, C-C ring vibrations
8,50	ν_{C-O-S}

v, stretching vibration.

varied with growth. Most of collagen fibrils were oriented parallel to the AC surface throughout the tissue at the age of 4 months. The fibril orientation changed obviously, however, with skeletal maturation. At the age of 21 months, the orientation of fibrils in RZ changed from parallel to perpendicular to the AC surface, as well as the collagen network anisotropy increasing significantly. Synchronously, the collagen content increased and its content distribution with cartilage depth varied during growth and maturation.

Yin's group applied FTIRI and polarization method to investigate the anisotropic structure change of collagen fibril of AC blocks fixed in formalin (27). The anisotropy of amide components became stronger with immersing extension of AC in formalin, and the amide I showed more remarkable anisotropy than amide II. It suggested that the formalin solution induced new crosslinks of collagen, which gradually strengthened the collagen fibril anisotropy.

FTIRI for content change of cartilage components

FTIRI has been used for the research on the component content since 2001 for bovine nasal cartilage (BNC) (28). Camacho's group (17,29) focused on the specific component distribution in AC by FTIRI and quantitatively analyzing the characteristic band intensity ratio. This was because the characteristic bands of principal components in cartilage overlapped each other so that distinctly affecting on the analysis on the principal component content and increasing difficulty of the quantitatively FTIRI research on content distribution. The studies on principal component content of AC and OA were subsequently done by second derivative

and peak area calculation (30,31), which achieved better outcomes in the variation of PG content.

The changes in the composition and distribution of principal component macromolecules in human OA cartilage were measured by using FTIRI (32). FTIRI-based PLS (partial least square) predicted the relatively low relative concentrations of principal components in induced OA cartilage. PG loss was correlated to histological Mankin scores, which mostly occurred in SZ and was strongly associated with the degeneration.

FTIRI was also combined with MRI and infrared fiber optic probe spectroscopy to research the changes of induced OA cartilage in a rabbit model by ligament transection and medial meniscectomy and to monitor disease progression (33). FTIRI on AC sections disclosed that PG content of the OA cartilage was significantly lost 2 and 4 weeks post-surgery, as well as collagen fibril orientation changing during the same period. Compared with control cartilage, no significant changes happened in collagen content, although collagen integrity varied 2 and 10 weeks post-surgery (33). However, collagen degraded in SZ at the end stage of OA (Mankin score 8–12) (32).

Principal component regression (PCR) algorithm was combined FTIRI to quantitatively detect collagen and PG concentrations in BNC (34). These PCR-determined percent concentrations of principal components were in agreement with the results detected biochemically using an enzyme digestion assay, suggesting that PG and collagen distributed homogeneously in BNC with approximate percent content. Based on the study, FTIRI with PCR was used for quantitative concentration predictions of collagen and PG in AC (16). The concentration ratio of collagen to PG was not lower than 60/40. The depth-dependent distributions of collagen and PG were inhomogeneous from surface to calcified zone. The highest content of collagen was in the SZ in dry tissue sections. The PG concentration showed a reversed trend as the collagen profile, namely, the lowest concentration being in the SZ and the maximum being at the middle tissue, which showed a consistent result of absolute PG concentration with that of MRI (Pearson correlation coefficient 0.98) when converted into the wet-weight condition (16).

The similar results of principal component distributions were obtained by using FTIRI with PLS (35). The reduction of the PG percent concentration at the surface tissue would be an early sign of the tissue degradation, associated with histological severity or OA level.

The reviews above further demonstrated that, as a

sensitive tool, FTIRI could accurately resolve and visualize the content distributions of principal component molecules in biological tissues. When FTIRI combined with other approaches (for example, chemometrics) could be helpful for improving our understanding of the complex processes in the variations of molecular composition and morphology in disease cartilage (16).

FTIRI for the monitoring and diagnosis of OA

West *et al.* (36) tried to evaluate the degenerative human AC by combining FTIRI with optical fiber probe. The optical fiber probe was contacted with AC surface to obtain its infrared spectra and visually grade normal or degraded. The pathological changes of OA cartilage surface were elucidated by the comparison of infrared spectral peak heights or areas. The study found that the IR absorption bands of type II collagen changed with degeneration of cartilage. Amide II/1,338 cm^{-1} area ratio increased and 1,238 cm^{-1} /1,227 cm^{-1} peak ratio decreased for the more impaired tissues. The similar changes were revealed in the FTIRI spectral analysis of the graded samples. Amide II, III and 1,338 cm^{-1} bands showed consistent spectral differences corresponding to those of Collins grades 1 and 3 cartilage, respectively. So these bands were not only related to type II collagen degeneration but might also predicted the extent of cartilage degeneration.

Hanifi *et al.* (37) sought to identify collagen type and other tissue components by FTIRI spectral evaluation of matrix components combined with PLS algorithm and the optical fiber probe. Type I and type II collagens came from different gene products, which existed in different tissues with different ratios. They displayed the different absorbance (peak area or height) under amide I, II and sugar bands. Additionally, there were some small differences in the second derivative spectra of them, showing as wavenumber shifts at amide I and II bands, CH₂ wagging and sugar bands. *Table 1* summarized the characteristic IR bands in cartilage and corresponding assignments. The research found that predominant type I collagen homogeneously distributed in bone and tendon; however type II collagen and PG distributed in normal cartilage while both type I and type II collagen were in repaired cartilage. The medial and lateral parts of the meniscus were mainly composed of type I and type II collagen, respectively.

FTIRI with PCR method were applied in quantitative determination of the principal component contents of AC at different OA stages by Yin *et al.* (38), as well as pathological

study. The PG loss increased gradually with the post-surgical duration, from 8 weeks, 12 weeks to 2 years post transection. At different surface locations and zones (SZ, TZ and RZ), PG showed different loss rule. The PG loss in the cartilage covered by meniscus was less than that of the cartilage uncovered by meniscus in OA and contralateral joints. The PG loss in the contralateral cartilage was less than that in the OA tibial cartilage. The PG loss in SZ under both OA and contralateral sides was the severest among the SZ, TZ and RZ. Therefore, FTIRI-PCR had potential to be developed in monitoring the injury, predicting disease progression, and repair of OA.

On the other hand, FTIRI combined with several chemometrics approaches that included PLS-discriminant analysis (PLS-DA) (39) and principal component analysis (PCA)-Fisher discriminant analysis (FDA) (40) was applied to identify healthy and OA cartilages. In the calibration and prediction groups of the mixed healthy and OA cartilage spectra, the identifying accuracies of PLS-DA were 100% and 90.24% (39), respectively, as well as FDA with accuracies of 94% and 86.67% (40). PCA prior to FDA was performed to decompose the IR spectral matrix into informative principal component matrices.

The same datasets were selected for comparing PLS-DA with PCA-FDA (41). Based on the different discriminant mechanism, the discriminant accuracy (96%) of PCA-FDA with high convenience was slightly higher than that of PLS-DA. Both integrated technologies of FTIRI-PLS-DA and FTIRI-PCA-FDA had great potential and could be used for clinical *in situ* monitoring of the OA early lesions and the repair of cartilage tissue.

Some limitations of FTIRI

FTIRI had some limitations in the study of cartilage and OA. First, the preparation process of cartilage samples was tedious and time-consuming, mainly in the tissue sections that were usually prepared by embedding them in the deformable substrate inside and being sectioned by Cryostat into slices with required thicknesses. On the other hand, the spectra of embedding agents, to some extent, interfered with those of cartilage components, further impacted on the analysis of principal component content. Second, the biopsy (even *in vitro*) samples from human body were harder to obtain, and therefore the number of analyzable samples and the generality of the research results were restricted. Third, expensive FTIRI microscopy instruments and their higher requirements on the measurement conditions limited their clinical application.

Conclusions and outlook

FTIRI could obtain simultaneously the spatial component (content) and microscopic structural information of biologic tissues with high spectral and spatial resolutions by scanning the surface morphology and collecting IR spectra, which achieved the visualization, micronization, high precision and high sensitivity in spectral analysis. In the cartilage studies, the accurate detection of principal component distribution and structure changes under high spatial resolution was being applied to the monitoring and diagnosis research of OA.

But so far, there were still some difficulties for FTIRI to be directly used in clinical monitoring and diagnosis of OA. The FTIRI combined with microfiber probe and other methods would be important development directions of clinical monitoring and diagnosis. On the other hand, the early monitoring of the tissue degradation and the repair process needs to be implemented as soon as possible, furthermore to reveal the pathogenesis of OA at molecular level, which were exactly capable to be carried out by using FTIRI with related methods in this regard.

FTIRI combined with other methods has potential to become a promising tool for the basic research and degeneration discrimination of cartilage specimen as well as the diagnosis of cartilage lesion at microscopic level (41). The FTIRI achievements will be significant for understanding the pathogenesis of OA at molecular level and improving effective prevention and therapy of joint diseases.

Acknowledgments

Funding: The authors in NUAA acknowledge (I) the National Natural Science Foundation of China (NSFC) (61378087, 61505079); (II) Natural Science Foundation of Jiangsu Province (BK20151478, BK20150752) for funding this work.

Footnote

Conflicts of Interest: All authors have completed the ICMJE uniform disclosure form (available at <http://dx.doi.org/10.21037/aoj.2018.01.04>). The authors have no conflicts of interest to declare.

Ethical Statement: The authors are accountable for all aspects of the work in ensuring that questions related to the accuracy or integrity of any part of the work are appropriately investigated and resolved.

Open Access Statement: This is an Open Access article distributed in accordance with the Creative Commons Attribution-NonCommercial-NoDerivs 4.0 International License (CC BY-NC-ND 4.0), which permits the non-commercial replication and distribution of the article with the strict proviso that no changes or edits are made and the original work is properly cited (including links to both the formal publication through the relevant DOI and the license). See: <https://creativecommons.org/licenses/by-nc-nd/4.0/>.

References

1. Hu JC, Athanasiou KA. Structure and function of articular cartilage. In: An YH, Martin KL. editors. Handbook of histology methods for bone and cartilage. Totowa(New Jersey): Humana Press, 2003:73-95.
2. Mow VC, Gu WY, Chen FH. Structure and function of articular cartilage and meniscus. In: Mow VC, Huijskes R. editors. Basic Orthopaedic Biomechanics and Mechanobiology. Philadelphia: Lippincott Williams & Wilkins, 2005:181-258.
3. Mow VC, Guo XE. Mechano-electrochemical properties of articular cartilage: their inhomogeneities and anisotropies. *Annu Rev Biomed Eng* 2002;4:175-209.
4. Rédini F. Structure and regulation of articular cartilage proteoglycan expression. *Pathol Biol (Paris)* 2001;49:364-75.
5. Buckwalter JA, Mankin HJ. Articular Cartilage. Part I: Tissue design and chondrocyte-matrix interactions. *J Bone Joint Surg Am* 1997;79:600-11.
6. Wilson W, Huyghe JM, van Donkelaar CC. Depth-dependent compressive equilibrium properties of articular cartilage explained by its composition. *Biomech Model Mechanobiol* 2007;6:43-53.
7. Brandt KD, Mankin HJ, Shulman LE. Workshop on etiopathogenesis of osteoarthritis. *J Rheumatol* 1986;13:1126-60.
8. Kiviranta I, Jurvelin J, Tammi M, et al. Microspectrophotometric quantitation of glycosaminoglycans in articular cartilage sections stained with Safranin O. *Histochemistry* 1985;82:249-55.
9. Xia Y, Zheng SK, Bidthanapally A. Depth-dependent profiles of glycosaminoglycans in articular cartilage by microMRI and histochemistry. *J Magn Reson Imaging* 2008;28:151-7.
10. Zheng S, Xia Y, Bidthanapally A, et al. Damages to the extracellular matrix in articular cartilage due to cryopreservation by microscopic magnetic resonance

- imaging and biochemistry. *Magn Reson Imaging* 2009;27:648-55.
11. Chen SS, Falcovitz YH, Schneiderman R, et al. Depth-dependent compressive properties of normal aged human femoral head articular cartilage: relationship to fixed charge density. *Osteoarthritis Cartilage* 2001;9:561-9.
 12. Xia Y, Moody JB, Burton-Wurster N, et al. Quantitative in situ, correlation between microscopic MRI and polarized light microscopy studies of articular cartilage. *Osteoarthritis Cartilage* 2001;9:393-406.
 13. Xia Y, Ramakrishnan N, Bidthanapally A. The Depth-dependent Anisotropy of Articular Cartilage by Fourier-Transform Infrared Imaging (FTIRI). *Osteoarthritis Cartilage* 2007;15:780-8.
 14. Bonifacio A, Beleites C, Vittur F, et al. Chemical imaging of articular cartilage sections with Raman mapping, employing uni- and multi-variate methods for data analysis. *Analyst* 2010;135:3193-204.
 15. Lim NS, Hamed Z, Yeow CH, et al. Early detection of biomolecular changes in disrupted porcine cartilage using polarized Raman spectroscopy. *J Biomed Opt* 2011;16:017003.
 16. Yin J, Xia Y, Lu M. Concentration profiles of collagen and proteoglycan in articular cartilage by Fourier transform infrared imaging and principal component regression. *Spectrochim Acta A Mol Biomol Spectrosc* 2012;88:90-6.
 17. Camacho NP, West P, Torzilli PA, et al. FTIR microscopic imaging of collagen and proteoglycan in bovine cartilage. *Biopolymers* 2001;62:1-8.
 18. Bi X, Li G, Doty SB, et al. A novel method for determination of collagen orientation in cartilage by Fourier transform infrared imaging spectroscopy (FT-IRIS). *Osteoarthritis Cartilage* 2005;13:1050-8.
 19. Ramakrishnan N, Xia Y, Bidthanapally A, et al. Determination of zonal boundaries in articular cartilage using infrared dichroism. *Appl Spectrosc* 2007;61:1404-9.
 20. Xia Y, Alhadlaq H, Ramakrishnan N, et al. Molecular and morphological adaptations in compressed articular cartilage by polarized light microscopy and Fourier-transform infrared imaging. *J Struct Biol* 2008;164:88-95.
 21. Lee JH, Xia Y. Quantitative zonal differentiation of articular cartilage by microscopic magnetic resonance imaging, polarized light microscopy, and Fourier-transform infrared imaging. *Microsc Res Tech* 2013;76:625-32.
 22. Ramakrishnan N, Xia Y, Bidthanapally A. Polarized IR microscopic imaging of articular cartilage. *Phys Med Biol* 2007;52:4601-14.
 23. Ramakrishnan N, Xia Y, Bidthanapally A. Fourier-transform infrared anisotropy in cross and parallel sections of tendon and articular cartilage. *J Orthop Surg Res* 2008;3:48.
 24. Xia Y, Mittelstaedt D, Ramakrishnan N, et al. Depth-dependent anisotropies of amides and sugar in perpendicular and parallel sections of articular cartilage by Fourier transform infrared imaging (FTIRI). *Microsc Res Tech* 2011;74:122-32.
 25. Yin JH, Xia Y, Ramakrishnan N. Depth-dependent anisotropy of proteoglycan in articular cartilage by Fourier transform infrared imaging. *Vib Spectrosc* 2011;57:338-41.
 26. Rieppo J, Hyttinen MM, Halmesmaki E, et al. Changes in spatial collagen content and collagen network architecture in porcine articular cartilage during growth and maturation. *Osteoarthritis Cartilage* 2009;17:448-55.
 27. Wu YC, Zhang XX, Mao ZH, et al. Study on the anisotropy of collagenous fibers in articular with infrared imaging. *Spectrosc Spect Anal* 2016;36:2071-75.
 28. Potter K, Kidder LH, Levin IW, et al. Imaging of collagen and proteoglycan in cartilage sections using Fourier transform infrared spectral imaging. *Arthritis Rheum* 2001;44:846-55.
 29. Bi X, Yang X, Bostrom MP, et al. Fourier transform infrared imaging spectroscopy investigations in the pathogenesis and repair of cartilage. *Biochim Biophys Acta* 2006;1758:934-41.
 30. Rieppo L, Saarakkala S, Närhi T, et al. Application of second derivative spectroscopy for increasing molecular specificity of Fourier transform infrared spectroscopic imaging of articular cartilage. *Osteoarthritis Cartilage* 2012;20:451-9.
 31. Rieppo L, Närhi T, Helminen HJ, et al. Infrared spectroscopic analysis of human and bovine articular cartilage proteoglycans using carbohydrate peak or its second derivative. *J Biomed Opt* 2013;18:097006.
 32. David-Vaudey E, Burghardt A, Keshari K, et al. Fourier transform infrared imaging of focal lesions in human osteoarthritic cartilage. *Eur Cell Mater* 2005;10:51-60.
 33. Bi X, Yang X, Bostrom MP, et al. Fourier transform infrared imaging and MR microscopy studies detect compositional and structural changes in cartilage in a rabbit model of osteoarthritis. *Anal Bioanal Chem* 2007;387:1601-12.
 34. Yin J, Xia Y. Macromolecular concentrations in bovine nasal cartilage by Fourier transform infrared imaging and principal component regression. *Appl Spectrosc* 2010;64:1199-208.

35. Zhang XX, Mao ZH, Yin JH, et al. Determination of collagen and proteoglycan concentration in osteoarthritic and healthy articular cartilage by Fourier transform infrared imaging and partial least square. *Vib Spectrosc* 2015;78:49-53.
36. West PA, Bostrom MP, Torzilli PA, et al. Fourier transform infrared spectral analysis of degenerative cartilage: an infrared fiber optic probe and imaging study. *Appl Spectrosc* 2004;58:376-81.
37. Hanifi A, Mccarthy H, Roberts S, et al. Fourier transform infrared imaging and infrared fiber optic probe spectroscopy identify collagen type in connective tissues. *PLoS One* 2013;8:e64822.
38. Yin J, Yang X. Proteoglycan concentrations in healthy and diseased articular cartilage by Fourier transform infrared imaging and principal component regression. *Spectrochim Acta A Mol Biomol Spectrosc* 2014;133:825-30.
39. Zhang XX, Yin JH, Mao ZH, et al. Discrimination of healthy and osteoarthritic articular cartilages by Fourier transform infrared imaging and partial least squares-discriminant analysis. *J Biomed Opt* 2015;20:060501.
40. Mao ZH, Yin JH, Zhang XX, et al. Discrimination of healthy and osteoarthritic articular cartilage by Fourier transform infrared imaging and Fisher's discriminant analysis. *Biomed Opt Express* 2016;7:448-53.
41. Mao ZH, Wu YC, Zhang XX, et al. Comparative study on identification of healthy and osteoarthritic articular cartilages by Fourier transform infrared imaging and chemometrics methods. *J Innov Opt Health Sci* 2017;10:1650054.

doi: 10.21037/aoj.2018.01.04

Cite this article as: Wang X, Zhai M, Zhao Y, Yin J. A review of articular cartilage and osteoarthritis studies by Fourier transform infrared spectroscopic imaging. *Ann Joint* 2018;3:9.